

## Radiation damage in NaCl. III. Melting phenomena of sodium colloids

J. Seinen, J. R. W. Weerkamp, J. C. Groote, and H. W. den Hartog

*Solid State Physics Laboratory, University Groningen, Nijenborgh 4, 9747 AG Groningen, The Netherlands*

(Received 4 June 1992; revised manuscript received 2 March 1994)

We report measurements on the melting behavior of colloids produced in irradiated NaCl. With differential scanning calorimetry (DSC) several latent-heat peaks near the melting temperature of pure bulk sodium metal have been detected. It appears that the total latent heat in these peaks is an accurate measure of the amount of damage in the crystal. Peak temperature and shape provide more detailed information about the properties of the colloids. The different melting temperature can be explained by differences in the typical sizes of the colloid, based on the theory for melting of small particles. This DSC technique provides a method to evaluate the production of radiation damage in detail without changing the properties of the damaged crystal.

### I. INTRODUCTION

Many different experimental techniques<sup>1-5</sup> have been used to study radiation damage in alkali halides, among which optical-absorption spectroscopy, as described in paper I (Ref. 6) and II,<sup>7</sup> is of particular importance. However, the technique is limited to relatively low irradiation doses (up to 3 Grad). Here we describe a nondestructive thermal analysis technique, which is particularly suitable for the analysis of sodium colloids in high-dose-irradiated NaCl.

The irradiation of alkali halides results in the aggregation of primary defects, forming higher-order clusters and finally colloids and dislocation loops. The results on high-dose irradiations ( $> 1$  Grad) show that the amount of colloidal sodium can reach a level of about 1 mol % at 10 Grad up to 10 mol % at doses higher than 100 Grad.<sup>8,9</sup> The optical density of such crystals is too high to be measured accurately ( $> 10\,000$  OD/cm). In case of heavily damaged crystals, the measurement of the stored energy (SE), which is released by recombining centers when the crystal is heated up to 500 °C, is frequently utilized. However, this thermal analysis method does not reveal much detailed information about the radiation products in the crystal and annihilates all the damage in the crystal for further analysis.

More appropriate for the investigation of heavily damaged crystals is the measurement of the latent heat (LH) needed for phase transitions in the colloids. Using differential scanning calorimetry (DSC) the melting of colloids is made visible by the appearance of several latent-heat peaks in the DSC scan.

Similar differential thermal analysis (DTA) experiments had been performed earlier by Lambert, Mazieres, and Guinier,<sup>10</sup> however, only on lithium colloids in neutron irradiated LiF. In our laboratory we measured a large number of NaCl crystals, varying in dose, dose rate, irradiation temperature, and dopant, demonstrating the wide scope of the experimental method for sodium colloids. The crystals were irradiated with 1.3-MeV electrons from a van de Graaff accelerator.<sup>11</sup> The crystals

were doped with different impurities, such as K, Li, F, Br, and mixed dopant KBF<sub>4</sub>, with concentrations chosen in accordance with the occurrence of the specific impurity in natural rocksalt.

In the results described below we will concentrate on the data of crystals doped with 0.1 mol % K irradiated at 100 Mrad/h with doses varying from 5 to 150 Grad. The irradiation temperature varied in the range of 20 to 150 °C. We will briefly comment on the results of other types of rocksalt crystals to illustrate some of the most important features in connection with the latent-heat peaks.

### II. EXPERIMENTAL METHOD

Differential scanning calorimetry (DSC) is a very sensitive method to study phase transitions that are accompanied by thermal effects. This technique provides the heat flow needed to raise a sample in temperature at a constant rate.

The DSC apparatus operates as a thermal-null system. The irradiated sample and an unirradiated reference crystal are placed inside two identical platinum-iridium microfurnaces. In order to measure the melting transition the samples are heated simultaneously from 40 to 150 °C with a rate of 10 °C/min. The melting of the colloids in the irradiated sample causes a temperature difference between the samples. This difference, detected with an accuracy of 0.1 °C, is minimized by an extra heatflow for the irradiated sample. In this way the latent heat needed to melt metallic colloids will appear as an endothermal peak in the detected heatflow.

A heat flow of less than 0.01 mW can be distinguished from the noise. Damage levels of about 1 mol % correspond with a few tenths of a milligram sodium metal in the irradiated samples of 40 mg. The latent heat associated with these amounts of Na is sufficient, given the heat of fusion of sodium 0.113 J/mg, to allow accurate measurements with the DSC. The heating rate of 10 °C/min as used in this investigation appears to be the most appropriate choice. Further decreasing the rate does not

show any differences in the peak pattern, except for an increasing noise. Increasing the heating rate tends to smooth the peak shape and causes a small shift of the peak positions (about 3°C if the heating rate is increased to 50°C/min).

The stored energy in the crystal is measured by heating the crystal to temperatures of typically 500°C with a rate of 150°C/min. During the DSC scan the sodium and chlorine aggregates dissociate and react back into NaCl. The energy release involved in this process can be detected as an exothermal peak in the heatflow. The area of the peak is an accurate measure of the total damage present in the sample. However, in contrast with the latent-heat measurement described above, the method destroys the products of radiation damage completely.

### III. OBSERVATIONS

In general the DSC signal associated with latent-heat effects shows two or three peaks, depending on the irradiation dose and temperature. The latent heat is obtained by integrating over the area of each peak in the DSC scan. The latent heat is measurable for samples, which had been irradiated at temperatures between 50 and 150°C, with a maximum amount at temperatures varying from 120°C at low doses to about 100°C at high doses. In Fig. 1 typical DSC scans of crystals doped with 0.1 mol % K are presented, showing the development of the melting peak pattern for increasing doses.

Two narrow peaks at rather fixed temperatures, peak 1 at 80°C (P1) and peak 2 at 92°C (P2) with a full width at half maximum (FWHM) of about 5°C, are already present at relatively low doses, when the amount of latent heat is just large enough to be detected (at a dose of 5 Grad). The peak patterns for other irradiation temperatures are similar, with an approximately constant ratio of the peak areas P2/P1. The area of peak 1 decreases slowly after 10 Grad, while peak 2 (the rest of the total area) increases. This can be seen from Fig. 2, which shows the partition of the latent heat over peaks 1 and 2 as function of the dose. The range of irradiation temperatures is restricted to the range where the damage production has a maximum efficiency. In order to evaluate the different peak areas we used a Gaussian peak fit program. Peak 1 is defined as the peak at 80°C, superimposed on the low-temperature flank of the more asymmetrically shaped peak 2, which could be fitted accurately by three Gaussian peaks.

A third peak (P3) at melting temperatures which may vary between 95 and 112°C is observed only at high doses (> 20 Grad), when a certain threshold damage level is reached (0.5–0.8J/g LH). Figure 3 shows that this condition is reached after about 25–30 Grad. Once peak 3 has appeared only the latent heat contained in peak 3 increases. This behavior is similar for all irradiation temperatures. This can be seen from Fig. 4, which shows the amount of latent heat contained in peak 3 as compared to the total latent heat for all the samples irradiated at temperatures between 20 and 150°C. With increasing doses the latent heat in peaks 1 and 2 decreases slowly and in some cases, at very high doses (> 100 Grad), only peak 3

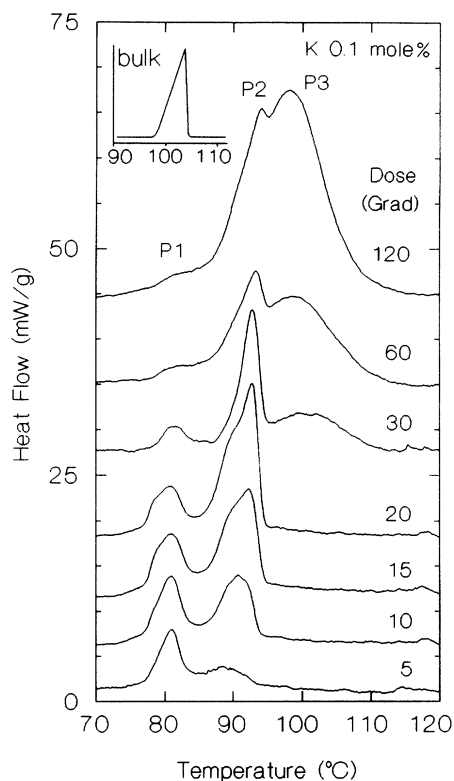


FIG. 1. Typical DSC scans of sodium colloids in heavily irradiated NaCl, doped with 0.1 mol % potassium, irradiated with a dose rate of 100 Mrad/h.  $T_{\text{irr}} = 100^\circ\text{C}$ , except for the 5 and 10 Grad samples, where  $T_{\text{irr}} = 120$  and  $110^\circ\text{C}$ . The total latent-heat values per gram NaCl are respectively, 0.25, 0.48, 0.63, 0.68, 0.70, 1.09, and 2.13 J/g. The inset shows the melting peak of bulk sodium.

is observed. The amount of latent heat reaches a level of about 3J/g after 150 Grad, which corresponds to about 7 mol % colloidal sodium (based on the latent heat of fusion of 0.113 J/mg for bulk sodium). The maximum production is in the range of irradiation temperatures around 100°C. At high irradiation temperatures (> 135°C), for which the damage production efficiency is

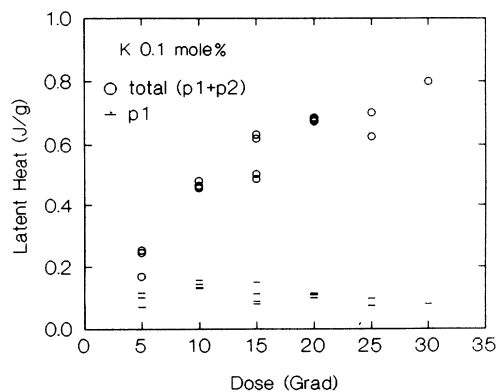


FIG. 2. The partition of the latent heat over peaks 1 and 2 as function of the dose for K 0.1 mol % doped crystals which did not show a third peak.  $T_{\text{irr}} = 100\text{--}130^\circ\text{C}$ .

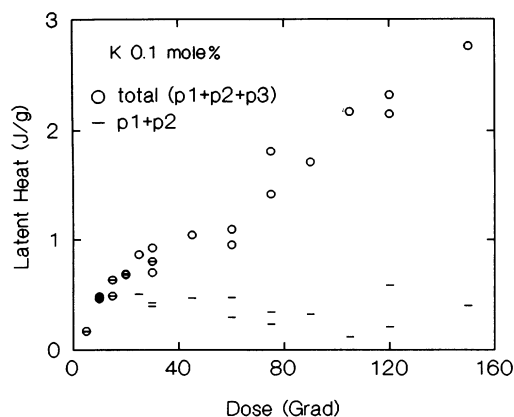


FIG. 3. The partition of the latent heat over peak 3 and peaks 1 and 2 as function of the dose for K 0.1 mol % doped crystals.  $T_{\text{irr}}=100\text{--}110^\circ\text{C}$ .

relatively low, the third peak has not been observed, although the threshold damage level was already reached. The peak can be very wide (FWHM up to  $20^\circ\text{C}$ ) and has a Gaussian shape.

Figure 1 shows that the peak shapes and temperatures deviate strongly from the melting peak observed for bulk sodium metal ( $97.8^\circ\text{C}$ ). None of the melting peaks can be associated with the melting of bulk sodium in irradiated NaCl. The bulk sodium peak is indeed found at about  $98^\circ\text{C}$  and can only be obtained in crystals with an excess amount of sodium after long term annealing at very high temperatures ( $>500^\circ\text{C}$ ).

Peak 1 and peak 2 are present for all the investigated dopants and concentrations, having the same dose dependence as described for the K 0.1 mol % doped crystals. The occurrence of peak 3 depends on the dopant of the crystal. For NaCl doped with varying concentrations potassium (0.001–1.0 mol %) a clearly distinguishable, Gaussian-shaped peak 3 arises, if the threshold level of 0.5 J/g LH is reached. For an impurity concentration of 0.01 mol % K the damage production at an irradiation

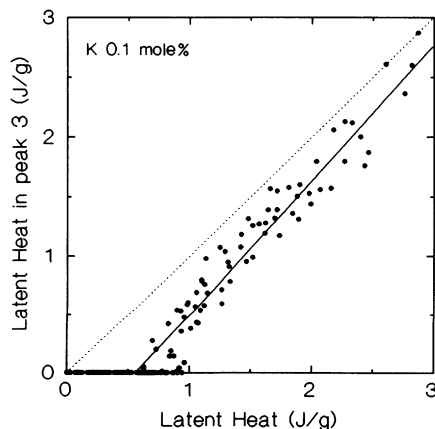


FIG. 4. The partial latent heat of peak 3 versus the total latent heat for K 0.1 mol % doped crystals. Typical peak patterns are shown in Fig. 1.

temperature of  $100^\circ\text{C}$  is about 25% lower than for 0.1 mol % K. In crystals with other dopants (Ba, mixed dopant  $\text{KBF}_4$ ) peak 3 has also been detected, showing up at about the same threshold level ( $0.4\pm 0.2$  J/g). In the case of  $\text{KBF}_4$  doped crystals the production of radiation damage was considerably higher ( $>5$  J/g LH after 150 Grad) than for other crystals. In the case of Li 0.05 mol % doped crystals a saturation of the damage production at an amount of 0.5 J/g LH has been observed after about 30 Grad, which prolonged at least up to 90 Grad (the crystals showing only melting peaks 1 and 2). Only at the highest doses a significant peak 3 has been observed for Li-doped crystals (at 150 Grad, 1 J/g LH). Usually, peak 3 is positioned at a temperature between  $95$  and  $115^\circ\text{C}$ , however, for F-doped crystals peak 3 has frequently been found at temperatures higher than  $120^\circ\text{C}$ .

A comparison of the latent heat and the stored-energy measurements performed in our laboratory on the same set of samples<sup>9</sup> makes clear that the total latent heat is a good measure for the amount of radiation damage in the crystal. Figure 5 shows that the total latent heat per gram NaCl contained in the melting peaks is proportional to the stored energy per gram NaCl: 1 J/g LH corresponds to 191 J/g SE. If the atomic specific heat of melting for bulk sodium of 0.0273 eV is still applicable for the colloidal sodium, we obtain a recombination energy associated with the *F*- and *H*-center recombination of  $5.3\pm 0.5$  eV. This value is close to the value found with optical-absorption spectroscopy  $6.2\pm 1.0$  eV<sup>7</sup> (Ref. 7) and is near the theoretical (about 5 eV)<sup>12,13</sup> and experimental (4.25 eV)<sup>14</sup> values given by other authors. The small offset in the stored energy of about 20 J/g is probably related to other damage forms, i.e., sodium structures which do not contribute to the latent heat, stress phe-

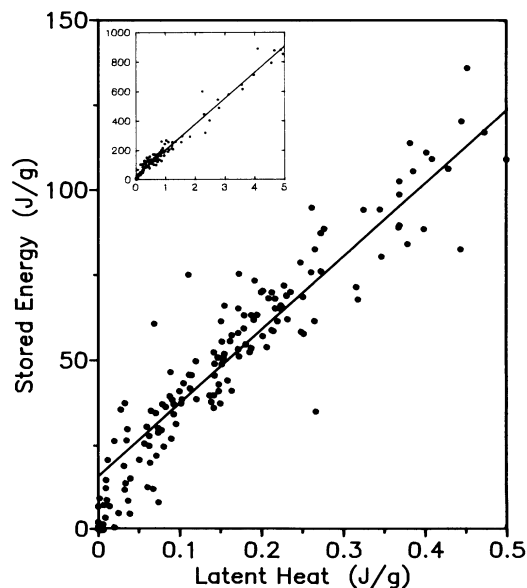


FIG. 5. The stored energy versus the latent heat for moderate damage levels, for different irradiation temperatures, doses and dopants. The inset shows a measurements of heavily damaged crystals for doses up to 150 Grad.

nomena or surface effects. The relatively large scatter of the data points near the origin reflect the accuracy of the latent-heat measurements at these damage levels.

In contrast with the corresponding experiments on LiF,<sup>10</sup> this experimental technique is not destructive for sodium colloids, probably because of the much lower temperatures required. The peak patterns are reproducible with high accuracy. Even after annealing at 300°C peak 1 and 2 are unchanged. The peak temperature of peak 3 decreases slightly, if the sample is heated to temperatures above 150°C. However, the peak area remains the same up to annealing temperatures of 250°C. These features make the DSC technique very useful as a method of analysis in combination with other experiments, such as Raman scattering and electron-spin resonance. A DSC scan of the melting peaks will be helpful to characterize the crystal and to see if the colloids have changed after an experiment.

#### IV. DISCUSSION

The melting peak patterns of the sodium colloids provide strong evidence that during irradiation at least three types of colloidal sodium are formed. We propose that the occurrence of different melting temperatures is due to the typical sizes of the particles involved. Numerous authors have considered the problem of melting of small particles as a function of the particle radius.<sup>15-17</sup> The classical treatment is based on the theory of Pawlow,<sup>18</sup> which is only valid for relatively large particles (> 1000 atoms). To obtain an expression which is also correct for smaller particles, Griffin and Andres<sup>19</sup> and Ross and Andres<sup>20</sup> have proposed the microscopic capillarity approximation. This approximation yields for the melting temperature  $T_m$  of a cluster with  $i$  particles:

$$\frac{T_m(i)}{T_m(\infty)} = 1 - A \left[ \frac{3}{i} \right]^{1/3} + \left[ A - 1 + \frac{T_m(3)}{T_m(\infty)} \right] \left[ \frac{3}{i} \right], \quad (1)$$

where

$$A = (12\pi)^{1/3} (\sigma_s v_s^{2/3} - \sigma_l v_l^{2/3}) / (lh_f). \quad (2)$$

Here  $T_m(\infty)$  is the bulk melting temperature of the solid,  $v_s$  and  $v_l$  are the atomic volumes of the solid and the liquid respectively,  $\sigma_s$  and  $\sigma_l$  are the respective bulk surface free energies, and  $lh_f$  is the heat of fusion. The melting temperature of a trimer  $T_m(3)$  is estimated by identifying the solid phase of a trimer as the state in which each atom is bound to the two other atoms and the liquid phase as the situation in which each atom is bound to only one other atom. Then the melting temperature of a trimer can be derived from the dissociation energy of a dimer  $\epsilon$ ,  $T_m(3) = 0.26\epsilon/k$ , where  $k$  is the Boltzman constant. This phenomenological approach yields good agreement with the available data for gold and argon clusters.<sup>21,22</sup>

This expression can be used to predict the melting temperature of small sodium clusters, however, the result is very sensitive to the bulk surface free energies of the solid and the liquid state. Unfortunately, there is disagreement among authors about the values of the bulk surface free

energies. We have used the values given by Miedema.<sup>23</sup> With  $\sigma_s = 0.228 \text{ J/m}^2$ ,  $\sigma_l = 0.200 \text{ J/m}^2$ ,  $v_s = 3.932 \times 10^{-29} \text{ m}^3$ ,  $v_l = 4.118 \times 10^{-29} \text{ m}^3$ ,  $lh_f = 4.375 \times 10^{-21} \text{ J}$ , and  $T_m(3) = 2408 \text{ K}$  ( $\epsilon = 0.8 \text{ eV}$ ) we have computed the melting curve in Fig. 6. However, to fit our experimental data we had to employ a correction factor of 0.16 for the parameter  $A$  in Eq. (2). This correction is probably related to the fact that the sodium particles are not surrounded by vacuum, but embedded in the NaCl matrix. The host matrix will modify the surface free energies of the particles. If we accept this choice, Fig. 6 suggests that peak 1 at 80°C can be associated with particles of 500–1000 atoms and peak 2 at 92°C with particles of more than 10000 atoms. Peak 3 is related to relatively small particles of 50–200 atoms. At these scales small changes in the number of atoms result in a large variation of the peak temperature, which explains the wide range of temperatures in which peak 3 has been found (95–140°C).

We should note, however, that other effects may be involved. Based on x-ray-diffraction studies, Lambert, and co-workers<sup>10,24</sup> attributed two latent-heat peaks in irradiated LiF to the melting of different crystal structures (bcc and fcc clusters). In agreement with this concept a possible explanation of the different melting peaks could be that the sodium at the surface of the colloid has an fcc structure, due to its interaction with the surrounding NaCl matrix. This interfacial colloid melts at a lower temperature than the inner sodium atoms, which have no interaction with the matrix.

Even without knowing the characteristic size and shape of the colloids exactly, we can attempt to draw some conclusions about the processes that give rise to the appearance of the melting peaks. Since similar peak patterns have been found for lithium colloids in irradiated LiF [DTA (Ref. 10) and DSC experiments performed in our laboratory], the process which give rise to the different types of colloid seem to be of a general nature for irradiated alkali halides.

Possibly the following processes are involved in the

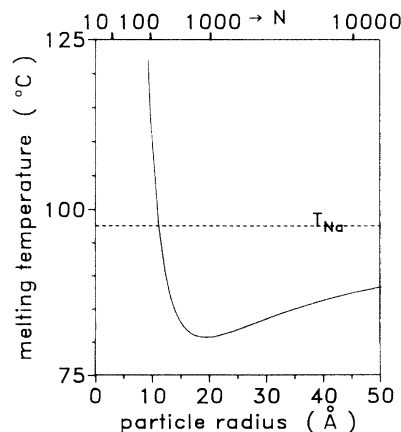


FIG. 6. The predicted melting temperature of small sodium particles as a function of the size of the particle. The curve is based on Eq. (1) with a correction factor of 0.16, for the parameter  $A$  in Eq. (2).

growth of colloids. In the early stages of the irradiation only two types of colloidal sodium are formed. The first form (peak 1) is determined by the diffusion of *F* centers. Some sort of open structure may be formed by diffusion-limited aggregation. Because this colloid structure can be heated far above the melting temperature of bulk sodium (up to 300 °C) and cooled down again without losing its characteristic latent-heat features, we conclude that this colloid structure is thermally stable. However, it is not unlikely that the freshly formed colloid is affected by the radiation induced lattice excitations within a few anion distances from the colloid. In this way the colloid will be transformed during irradiation into a configuration which is less sensitive to further excitations, i.e., a more compact structure (peak 2). This explains why peak 2 increases proportional to the dose, whereas peak 1 remains approximately constant. Such a transformation process is only related to the dose rate, such that the ratio P2/P1 between the peaks is independent of the irradiation temperature.

When the crystal is damaged very heavily by the irradiation, the damage production will change because of the changing crystal properties. An excitation only results in the creation of an *F-H* pair, if the primary defects are separated by many anion distances. Therefore one expects that at a certain damage level an effective creation of *F-H* pairs is not possible anymore, because the *F* and *H* center will be captured by the same damage form. For instance, if the dislocation line density becomes very high, due to the continuous capture of *H* centers, the

probability to capture both the *F* and the *H* center becomes very high. The new *H* center will settle down close to the dislocation line, whereas the new *F* center will immediately annihilate at the dislocation line, such that the net result is the annihilation of the created *F-H* pair. This idea has been introduced into a general model, which describes the nucleation and aggregation of colloids.<sup>25</sup> Such a process would result in a saturation of the radiation damage.

We expect that the damage form represented by melting peak 1 and 2 can be associated with a process leading to saturation as described above, which is determined by diffusion through the matrix. This would explain the saturation of this damage form in the case of Li-doped crystals. However, the K-doped crystals (and others) do not saturate with damage. The appearance of the third melting peak at latent heat levels of 0.5 J/g (about 1 mol % colloidal sodium) for specific dopants indicates that other processes become favorable in these crystals. Possibly diffusion along the dislocation lines becomes dominant and much smaller colloids are formed along the dislocation lines.

#### ACKNOWLEDGMENT

This work has been supported financially by the Dutch Ministry of Economic Affairs, as a part of the OPLA (OPberging te LAnd) research programme, in order to investigate the disposal of high level nuclear waste in salt domes.

- 
- <sup>1</sup>G. H. Jenks, E. Sonder, C. D. Bopp, J. R. Walton, and S. Lindenbaum, *J. Phys. Chem.* **79**, 871 (1975).  
<sup>2</sup>P. W. Levy, J. M. Loman, K. J. Swyler, and D. R. Dougherty, *Radiat. Eff.* **72**, 303 (1983).  
<sup>3</sup>P. W. Levy, K. J. Swyler, and R. W. Klaffky, *J. Phys. Colloq.* **41**, C6-344 (1980).  
<sup>4</sup>A. E. Hughes, *Radiation Eff.* **74**, 57 (1983).  
<sup>5</sup>J. C. Groote, J. Seinen, J. R. W. Weerkamp, and H. W. den Hartog, *Radiat. Eff. Def. Solids* **119-121** 925 (1991).  
<sup>6</sup>J. R. W. Weerkamp, J. C. Groote, J. Seinen, and H. W. den Hartog, this issue, paper I, *Phys. Rev. B* **50**, 9781 (1994).  
<sup>7</sup>J. Seinen, J. C. Groote, J. R. W. Weerkamp, and H. W. den Hartog, this issue, paper II, *Phys. Rev. B* **50**, 9787 (1994).  
<sup>8</sup>G. H. Jenks and C. D. Bopp (unpublished).  
<sup>9</sup>J. R. W. Weerkamp, J. C. Groote, J. Seinen, and H. W. den Hartog (unpublished).  
<sup>10</sup>M. Lambert, C. Mazières, and A. Guinier, *J. Phys. Chem. Solids* **18**, 129 (1961).  
<sup>11</sup>J. C. Groote, J. R. W. Weerkamp and H. W. den Hartog, *Meas. Sci. Technol.* **2**, 1187 (1991).  
<sup>12</sup>A. E. Hughes, *Comm. Sol. St. Phys.* **8**, 83 (1978).  
<sup>13</sup>K. M. Diller (unpublished).  
<sup>14</sup>G. H. Jenks, E. Sonder, C. D. Bopp, J. R. Walton, and S. Lindenbaum, *J. Phys. Chem.* **79**, 871 (1975).  
<sup>15</sup>H. Reiss and I. B. Wilson, *J. Colloid Sci.* **3**, 551 (1948).  
<sup>16</sup>P. R. Couchman and W. A. Jesser, *Nature (London)* **269**, 481 (1977).  
<sup>17</sup>M. Hasegawa, K. Hoshino, and M. Watabe, *J. Phys. F* **10**, 137 (1980).  
<sup>18</sup>P. Pawlow, *Z. Phys. Chem.* **65**, 545 (1909).  
<sup>19</sup>G. L. Griffin and R. P. Andres, *J. Chem. Phys.* **71**, 2522 (1979).  
<sup>20</sup>J. Ross and R. P. Andres, *Surf. Sci.* **106**, 11 (1981).  
<sup>21</sup>Ph. Buffat and J. P. Borel, *Phys. Rev. A* **13**, 2287 (1976).  
<sup>22</sup>J. R. Sambles, *Proc. R. Soc. London Ser. A* **324**, 339 (1971).  
<sup>23</sup>A. R. Miedema and J. A. den Broeder, *Z. Metallk.* **70**, 14 (1979).  
<sup>24</sup>A. E. Hughes and S. C. Jain, *Adv.* **28/6** 717 (1979).  
<sup>25</sup>J. Seinen, J. C. Groote, J. R. W. Weerkamp, and H. W. den Hartog, *Rad. Eff. Def. Solids* **124**, 325 (1992).